Fuel 337 (2023) 127178

Contents lists available at ScienceDirect

Fuel

journal homepage: www.elsevier.com/locate/fuel

Full Length Article

Gaseous fueling of an adapted commercial automotive spark-ignition engine: Simplified thermodynamic modeling and experimental study running on hydrogen, methane, carbon monoxide and their mixtures

José Carlos Urroz [a], Pedro M. Diéguez [a,*], Gurutze Arzamendi [b], Miguel Arana [b], Luis M. Gandía [b,*]

[a] Departamento de Ingeniería, Universidad Pública de Navarra (UPNA), Arrosadia Campus, 31006 Pamplona, Spain
[b] Institute for Advanced Materials and Mathematics (INAMAT²), Departamento de Ciencias, Universidad Pública de Navarra (UPNA), Arrosadia Campus, 31006 Pamplona, Spain

ARTICLE INFO

Keywords:
Gaseous fuels
Hydrogen
Internal combustion engine
Methane
Thermodynamic modelling

ABSTRACT

In the present work, methane, carbon monoxide, hydrogen and the binary mixtures 20 % CH_4–80 % H_2, 80 % CH_4–20 % H_2, 25 % CO–75 % H_2 (by volume) were considered as fuels of a naturally aspirated port-fuel injection four-cylinder Volkswagen 1.4 L spark-ignition (SI) engine. The interest in these fuels lies in the fact that they can be obtained from renewable resources such as the fermentation or gasification of residual biomasses as well as the electrolysis of water with electricity of renewable origin in the case of hydrogen. In addition, they can be used upon relatively easy modifications of the engines, including the retrofitting of existing internal combustion engines. It has been found that the engine gives similar performance regardless the gaseous fuel nature if the air–fuel equivalence ratio (λ) is the same. Maximum brake torque and mean effective pressure values within 45–89 N·m and 4.0–8.0 bar, respectively, have been obtained at values of λ between 1 and 2 at full load, engine speed of 2000 rpm and optimum spark-advance. In contrast, the nature of the gaseous fuel had great influence upon the range of λ values at which a fuel (either pure or blend) could be used. Methane and methane-rich mixtures with hydrogen or carbon monoxide allowed operating the engine at close to stoichiometric conditions (i.e. $1 < \lambda < 1.5$) yielding the highest brake torque and mean effective pressure values. On the contrary, hydrogen and hydrogen-rich mixtures with methane or carbon monoxide could be employed only in the very fuel-lean region (i.e. $1.5 < \lambda < 2$). The behavior of carbon monoxide was intermediate between that of methane and hydrogen.

The present study extends and complements previous works in which the aforementioned fuels were compared only under stoichiometric conditions in air ($\lambda = 1$). In addition, a simple zero-dimensional thermodynamic combustion model has been developed that allows describing qualitatively the trends set by the several fuels. Although the model is useful to understand the influence of the fuels properties on the engine performance, its predictive capability is limited by the simplifications made.

1. Introduction

There is an urgent need for adapting our energy system to the current situation of climate emergency. An important achievement of the COP26 UN Climate Conference held in Glasgow in November 2021 has been the adoption of the Paris Agreement Rulebook, thus maintaining the upper end of ambition of that important deal. Accordingly, we are now at the beginning of a critical decade to adopt decided actions in order to limit global warming below 1.5 °C, by means of deep and sustained reductions in global greenhouse gases (GHGs) emissions to the atmosphere. The goals are reducing global CO_2 emissions by 45 % by 2030 relative to the 2010 level, and to net zero around 2050, as well as deep reductions in other GHGs [1].

Mobility of people and goods through easy access to a wide variety of transport means (road, rail, shipping and aviation) is one of the distinctive features of the modern society. The fact that transport depends almost exclusively on fuels derived from oil makes a priority to decarbonize this sector. Indeed, energy consumption by the transport sector amounted in 2019 up to 120,972 EJ (2890 Gtoe), reaching 29 %

* Corresponding authors.
E-mail addresses: pmde@unavarra.es (P.M. Diéguez), lgandia@unavarra.es (L.M. Gandía).

https://doi.org/10.1016/j.fuel.2022.127178
Received 23 June 2022; Received in revised form 1 December 2022; Accepted 14 December 2022
Available online 22 December 2022

Nomenclature

AF	Mass air–fuel ratio
AF_{stoich}	Stoichiometric mass air–fuel ratio
BMEP	Brake mean effective pressure (bar)
BSFC	Brake specific fuel consumption (g/kW·h)
BT	Brake torque (N·m)
BTDC	Before top dead center
FCEVs	Fuel cell electric vehicles
GHGs	Greenhouse gases
$h(T)$	Specific enthalpy (J/mol)
h_f^0	Specific enthalpy of formation at reference conditions (J/mol)
$\Delta h(T)$	Specific enthalpy change with respect to the reference state (J/mol)
H2ICEs	Hydrogen-fueled internal combustion engines
ICEs	Internal combustion engines
LCVs	Light commercial vehicles
LHV	Lower heating value (MJ/kg)
LPG	Liquefied petroleum gas
MBP	Maximum brake power (kW)
MBT	Maximum brake torque (N·m)
n_e	Moles of product e (mol)
n_i	Moles of reactant i (mol)
p_a	Pressure in the intake manifold (bar)
p_e	In-cylinder pressure after fuel combustion at constant volume (bar)
p_i	In-cylinder pressure at the end of the compression stroke (bar)
P	Number of products
PFI	Port-fuel injection
r_c	Cylinder compression ratio
R	Number of reactants
SA	Spark advance (° BTDC)
SI	Spark-ignition
T	Temperature (K)
T_a	Temperature in the intake manifold (K)
T_e	In-cylinder temperature after fuel combustion at constant volume (K)
T_i	In-cylinder temperature at the end of the compression stroke (K)
TDC	Top dead center
$u(T)$	Specific internal energy (J/mol)
WOT	Wide open throttle
α	Stoichiometric coefficient for hydrogen (Eq. A2)
β	Stoichiometric coefficient for methane (Eq. A2)
γ	Stoichiometric coefficient for carbon monoxide (Eq. A2)
δ	Stoichiometric coefficient for nitrogen (Eq. A2)
ε	Stoichiometric coefficient for carbon dioxide (Eq. A2)
λ	Air-fuel equivalence ratio

of the world total energy demand. Oil products provided up to 91.3 % of this vast amount of energy. Other sources consisted in natural gas (4.1 %), biofuels and waste (3.3 %), and other renewables and electricity (1.2 %) [2]. As for the GHGs emissions from transport, they consisted almost exclusively in CO_2 (8.5 Gt) that represent 16.2 % of the global (52.4 Gt CO_2 equivalent, excluding land use change contributions) [3,4].

Most efforts to decarbonize the transport sector are being directed towards its electrification. This will require overcoming the unique challenges of achieving widespread availability of cheap, safe, durable, powerful, environmentally friendly and rapid to recharge batteries, and greatly increasing the capacity, usability and manageability of the grid to provide sufficient electricity of renewable origin. This strategy is complemented with the expected use of fuel cell electric vehicles (FCEVs) fed with renewable hydrogen for some specific vehicle segments.

There are big synergies between renewable electricity and hydrogen produced by means of water electrolysis [5]. Hydrogen production, storage, distribution and use has capacity to provide the required flexibility to an electric grid fed by a power system largely based on intermittent sources like the conventional renewables (solar and wind power). This can be accomplished by hydrogen acting as a buffer to surplus generation and allowing seasonal balancing of electricity production capacity and demand [6]. As a result, renewable hydrogen is being regarded as a key element of the future energy system because it has potential to decarbonize the most hardly electrifiable sectors [7]. According to the IRENA's Transforming Energy Scenario, hydrogen of various origins could supply about 29 EJ of global energy demand by 2050. The transport sector would be the second largest user of renewable hydrogen with 4 EJ (95.5 Mtoe) consumed per year by 2050 [8]. Whereas IRENA's predictions lead to the use of FCEVs in heavy-duty trucks for heavier freight transport, Hydrogen Europe highlights the big potential for emissions reduction offered by the segment of light commercial vehicles (LCVs). Hydrogen Europe also claims the legislators for including system efficiency and technology neutrality as principles to revise a regulation that in the EU currently tends to favor battery electric vehicles [9]. According to the Hydrogen Roadmap Europe, the deployment of FCEVs in the short-term is most attractive for commercial fleets and large passenger cars, vans, buses and trucks, where their advantages are most relevant [10].

Important features of hydrogen are that, in addition to an energy carrier, it is also a feedstock and a fuel. Main expected applications are in industry (iron and steel industries, chemicals including ammonia manufacture and high-temperature heat production). As a fuel, hydrogen can be burned in the internal combustion engines (ICEs) that have mainly sustained the development of the transportation sector over the last century [11]. Technical advancements and stringent environmental regulations have made that, at present, these engines achieve reasonably high energy efficiencies. In addition, they are very robust, relatively cheap and they are plentifully fabricated and used worldwide. Both spark-ignition (gasoline) and compression-ignition (diesel) engines can be adapted to run on gaseous fuels without requiring complex modifications [12] though onboard hydrogen storage and hydrogen infrastructure are more challenging issues [13,14]. Overall, current ICEs have great capacity to boost the decarbonization of the transportation sector by introducing renewable hydrogen as their fuel. Furthermore, it has been shown that blending hydrogen with other gases such as e.g., methane or even residual gases, is beneficial to make up for some characteristics of gaseous hydrogen such as its low volumetric energy density [15] or its tendency to suffer from anomalous combustion phenomena [16]. This opens the door to the combined use in ICEs of hydrogen and other renewable resources such as the biomethane [15] that can be obtained from biogas [17], the bio-syngas produced from the gasification or pyrolysis of biomass [18], or some relevant gaseous waste streams such as coke oven gas [19].

Our group has been working on the use of hydrogen in spark-ignition (SI) ICEs for over 15 years. All this work has been performed with commercial engines that were adapted to run on gaseous fuels to demonstrate the feasibility and high readiness level of the technology for stationary [20] and mobile [21] applications. As for automotive applications, a naturally aspirated port-fuel injection (PFI) four-cylinder Volkswagen 1.4 L SI engine was used [22,23]. Other recent works in this field are the studies performed by Fischer et al. with a 1 L three-cylinder engine from Ford Werke GmbH fueled with hydrogen [24], and by Kravos et al. with a four-cylinder 2.237 L Toyota 4Y-E engine

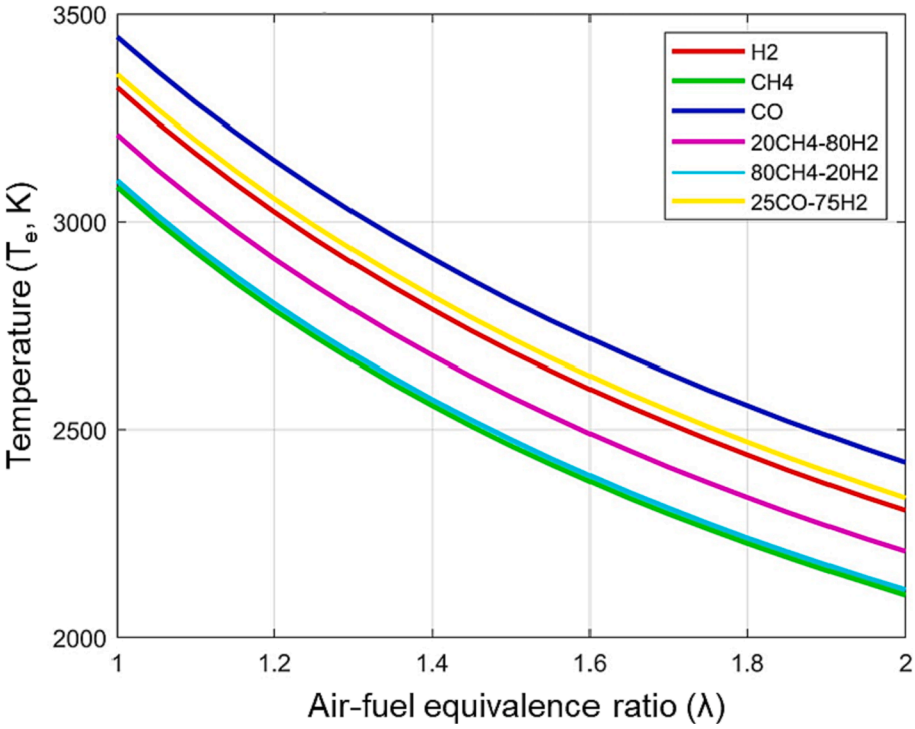

Fig. 1. Temperature of the combustion products according to Eq. A(4) (see the Appendix) as a function of the air–fuel equivalence ratio for the fuels indicated.

designed to run on LPG, natural gas and gasoline [25].

In this paper, we present the results of a study on the use of hydrogen, methane and carbon monoxide, and some of their mixtures as fuels of a commercial automotive engine. These compounds can be found in pure form or as mixtures of varying composition in alternative gaseous fuels (hydrogen and syngas [26], biogas [27], natural gas [28,29], and coke oven gas [30]). The general objective is to investigate the factors responsible for the different performance of the engine when fed with these gases aiming at generating knowledge useful to formulate alternative fuels that can help to decarbonize the transportation sector. To that end, a thermodynamic analysis is first conducted to assess the effects of the main physicochemical properties of the investigated compounds on their performance as fuels. Then, the performance of a commercial Volkswagen Polo 1.4 L PFI SI engine running on methane, carbon monoxide, hydrogen and binary mixtures thereof (20 % CH_4–80 % H_2, 80 % CH_4–20 % H_2, 25 % CO–75 % H_2) is investigated. The results are qualitatively compared with the theoretical predictions.

2. Thermodynamic analysis

The field of modeling and simulation of thermal engines power cycle has evolved considerably over the last years and has significantly contributed to the recent developments of ICEs. The models developed so far describe with different level of detail the physicochemical processes and the stages involved in the engine power cycle. They range from the thermodynamic zero-dimensional, multi-zone, and quasi-dimensional models to the more modern and sophisticated multi-dimensional models [31,32]. Improved detail and accuracy imply higher mathematical complexity and computational effort so, obviously, the type of model must be suitably selected according to the purpose and scope of the investigation.

As concerns the present study, a simplified first-law zero-dimensional model has been used to assess the influence of the most relevant thermophysical and physicochemical properties of methane, carbon monoxide and hydrogen on their performance as fuels of a SI engine. The influence of the corresponding air–fuel mixtures composition (i.e., mass air–fuel ratio (AF) and air–fuel equivalence ratio (λ)) has been also investigated. Within this context, the comprehensive work carried out by Caton [32,33] stands out among the previous research published on this topic. This author investigated the performance as fuels of methane, carbon monoxide and hydrogen from the perspective of the first and second laws of thermodynamics. Propane, hexane, isooctane, methanol and ethanol were also considered to study a wide variety of liquid and gaseous fuels. Moreover, from the point of view of the fuels' chemical nature, alkanes, oxygen containing molecules and hydrogen were considered. Focus was put on the thermal and exergy efficiencies of the individual fuels under stoichiometric conditions ($\lambda = 1$) as functions of engine speed and load. A thermodynamic model was developed for the whole engine cycle accounting for equilibrium composition for the burned gases, cylinder heat transfer, and combustion process described through a three-zone (unburned zone, adiabatic core burned zone, and boundary layer burned zone) combustion model [33]. In the present work, load has been set constant operating under wide open throttle (WOT), i.e., unthrottled conditions, whereas the performance of the pure fuels or some of their binary mixtures is investigated as function of λ using a simplified first-law model. Recognizing that the simplifying assumptions that are presented below significantly limit the predictive capacity of the model, it is believed that the results are useful as they complement those found in previous works by other authors. In addition, the conclusions drawn are supported by an experimental campaign performed with a commercial four-cylinder automotive engine.

2.1. Thermodynamic model formulation

It has been assumed that the combustion of all gaseous fuels and their mixtures is complete provided that the fuel–air mixture contains sufficient oxygen. In addition, the combustion reaction is assumed to be virtually instantaneous, so it takes place at a constant cylinder volume corresponding to top dead center (TDC) without heat exchange with the cylinder walls, resulting in an adiabatic process. Model formulation is described in the Appendix. All the thermodynamic properties have been calculated using the REFPROP program from NIST [34].

2.2. Basic first-law results

Fig. 1 shows the values of T_e as a function of the air–fuel equivalence ratio for the combustion of pure hydrogen, pure methane, pure carbon monoxide and the following binary mixtures: 20 % CH_4–80 % H_2, 80 % CH_4–20 % H_2 and 25 % CO–75 % H_2.

Values of $\lambda \geq 1$ have been considered, that is, stoichiometric and fuel-lean conditions. This choice is motivated by the advantages associated to the fuel-lean operating regime as concerns achieving high combustion and volumetric efficiencies [35]. Achieving that regime is made possible by the wider flammability limits of the gaseous fuels, particularly hydrogen and carbon monoxide, compared to the liquid fuels [36]. Table 1 includes the flammability limits in air and other relevant thermophysical properties of hydrogen, methane and carbon monoxide.

The adiabatic products temperature decreases as λ increases, which is a direct consequence of burning increasingly fuel-leaner mixtures. The relative order of the pure fuels with respect to the maximum adiabatic temperature is carbon monoxide > hydrogen > methane. This is the result of the combined effects of the system composition, the change of the total number of moles associated to the combustion reactions stoichiometry and the enthalpy change within the system, which can be approximated by the fuels energy content through their lower heating value (LHV). The combustion stoichiometry leads to the same molar (or volumetric) content of carbon monoxide and hydrogen under stoichiometric conditions (29.6 %), as shown in Fig. 2 (and Table 1). However, the molar LHV of carbon monoxide is higher than that of hydrogen (see Table 1), thus resulting in also higher adiabatic temperatures.

As for methane, its content under stoichiometric conditions (9.5 %) is 3.1 times lower than that of the other fuels whereas its molar LHV is between 2.8 (carbon monoxide) and 3.3. (hydrogen) times higher so that these effects almost offset each other. There is, however, a relevant difference between the combustion of these fuels since the combustion of carbon monoxide and hydrogen is accompanied by an equal decrease of the total number of moles whereas methane combustion takes place without changing the number of moles of the system. This result can be deduced from the general combustion reaction (see Eq. A(2) of the Appendix) that allows calculating the ratio $\sum_P n_e / \sum_R n_i$, i.e. the ratio between the total number of moles of products and reactants in the cylinder, or after and before the combustion reaction, respectively. Fig. 3 shows the evolution of that ratio as a function of λ for the complete combustion of the fuels considered in the present study.

It is apparent that carbon monoxide, hydrogen, and their binary mixture give identical results. The difference between the total number of moles of products and reactants (i.e. the molar contraction) decreases as λ increases due to the diluting effect of nitrogen and unreacted oxygen. Therefore, the extent of the molar contraction is maximum at $\lambda = 1$ and reaches ca. 15 %; then, it smoothly decreases to about 9 % at $\lambda = 2$. The molar contraction also decreases as the methane content in the binary mixture decreases until being zero for pure methane because methane combustion takes place without change of the total number of

Table 1
Selected thermophysical properties of the fuels indicated.

Fuel	$(AF)_{stoich}$ [33]	LHV (MJ/kg) [b] [33]	Specific heats ratio [34]	Flammability limits (vol.%) [a] [36]	Stoichiometric fuel concentration (vol.%) [a,c]
H_2	34.15	120 (242)	1.41	4–74	29.6
CH_4	17.17	50 (802)	1.30	5.0–15.0	9.5
CO	2.46	10.1 (283)	1.40	12.5–74.2	29.6

[a] Values for mixtures in air at standard conditions.
[b] Values in parentheses are given in MJ/kmol.
[c] Calculated from Eq. A(1) (see the Appendix).

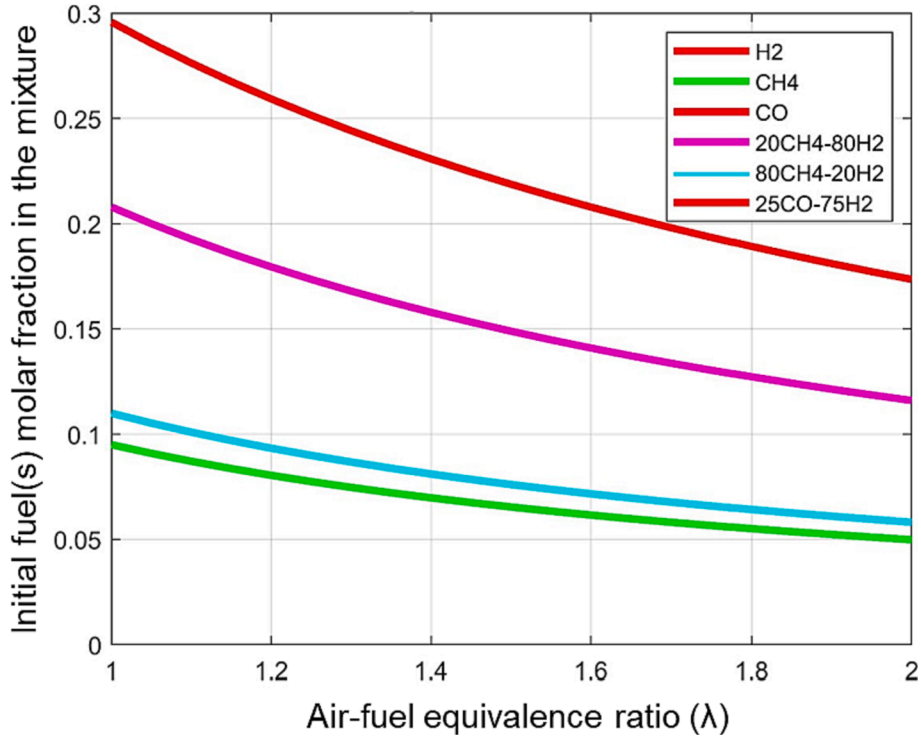

Fig. 2. Initial molar fraction of the fuel(s) indicated in the mixture with as function of the air–fuel equivalence ratio.

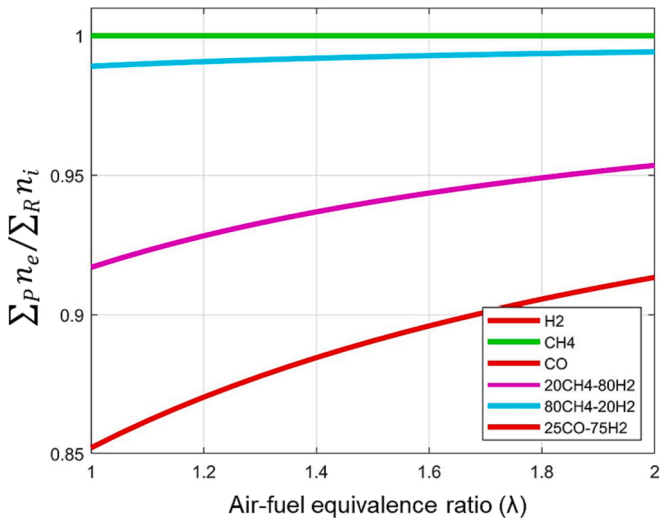

Fig. 3. Ratio between the total moles of products and reactants for the complete combustion of the fuel(s) indicated as function of the air–fuel equivalence ratio.

moles. Nevertheless, it is also necessary to consider possible changes of the specific heats. In this regard, the molar specific heats of the combustion products mixtures under stoichiometric conditions have been estimated to range between 43 kJ/(kmol·K) for methane combustion and 46 kJ/(kmol·K) for carbon monoxide combustion. This small difference will become even lower as at λ increases due to dilution in nitrogen and unreacted oxygen. Therefore, no significant effects can be expected from the changes of specific heats, whereas the molar contraction that takes place upon carbon monoxide and hydrogen combustion will also contribute to higher adiabatic temperatures compared to methane combustion.

As for the binary mixtures of fuels, the mixture 80 % CH_4–20 % H_2 gives rise to adiabatic temperatures close to that of pure methane over the whole range of λ values considered. This can be explained by the dominant effect of methane in these cases because the molar LHV of methane is much higher than that of hydrogen (see Table 1). In fact, it can be seen in Fig. 2 that the molar (or volumetric) methane content in the mixture 80 % CH_4–20 % H_2 with air under stoichiometric conditions ($\lambda = 1$) is 8.8 %, which is only slightly lower than that corresponding to burning pure methane under stoichiometric conditions in air (9.5 %). In contrast, the concentration of hydrogen is 2.2 %, i.e., 13.4 times lower than for pure hydrogen (29.6 %), also under stoichiometric conditions. As λ increases turning away from stoichiometric conditions with air, the differences as concerns the fuels content become even slightly lower (see Fig. 2) due to the diluting effect of nitrogen and oxygen in excess. In the case of the 20 % CH_4–80 % H_2 mixture, the methane concentration in the stoichiometric mixture with air decreases to 4.9 % whereas that of hydrogen increases up to 19.6 %. These values are compatible with a behavior intermediate between that of pure methane and pure hydrogen, as shown in Fig. 1.

Finally, in the case of the 25 % CO–75 % H_2 mixture, when combined with air in stoichiometric conditions, the resulting carbon monoxide and hydrogen concentrations are 7.4 % and 22.2 %, respectively. These values are 25 % and 75 % of the fuels concentrations corresponding to burning pure carbon monoxide and pure hydrogen (29.6 %), respectively. This gives rise to a behavior of that mixture that corresponds to the combination of the effects of the pure fuels weighted by the concentration in which each fuel is present.

Temperatures in Fig. 1 are much higher than the ones found in normal engine operation due to the assumptions made; particularly, by disregarding heat transfer to the cylinder walls. Despite this fact, the fuels are ranked in the same order than the one found by Caton according to the values of the enthalpy-averaged exhaust gas temperatures [33]. Under stoichiometric conditions, maximum enthalpy-averaged exhaust gas temperatures of ca. 1550 K (carbon monoxide), 1400 K (hydrogen) and 1275 K (methane) were calculated when modelling an eight-cylinder (V-8) SI automotive engine of 5.7 L and $r_c = 8.1$. According to Caton, these results are related to the heat transfer, exhaust gas temperatures and thermal efficiency for each fuel [33].

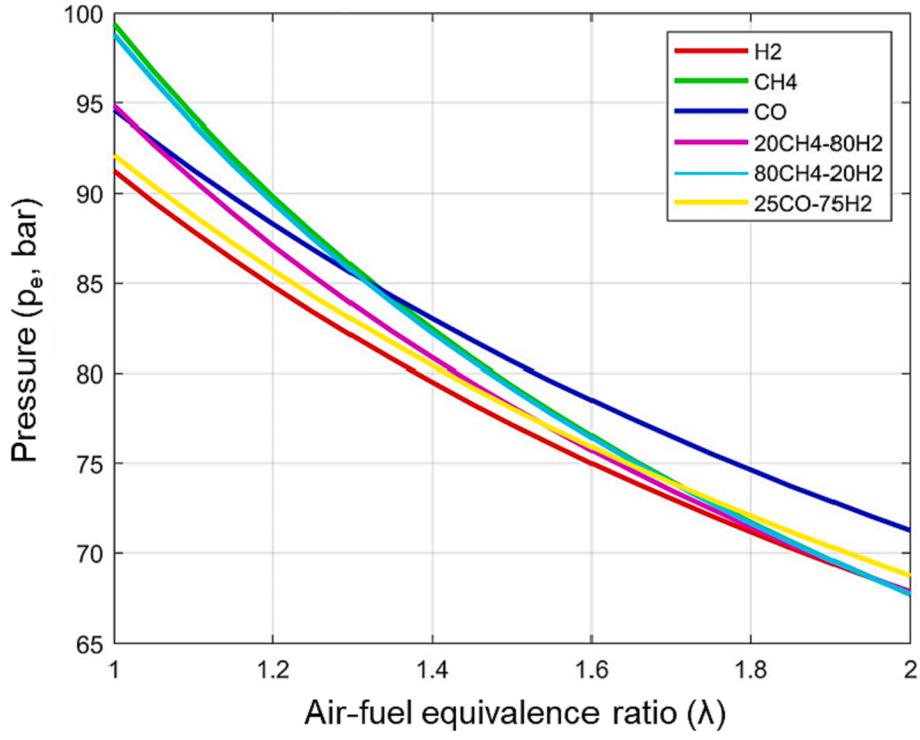

Fig. 4. Pressure of the combustion products according to Eq. A(7) (see the appendix) as a function of the air–fuel equivalence ratio for the fuels indicated.

Fig. 4 shows the values of p_e as function of the air–fuel equivalence ratio for the combustion of pure hydrogen, pure methane, pure carbon monoxide and the following binary mixtures: 20 % CH_4–80 % H_2, 80 % CH_4–20 % H_2 and 25 % CO–75 % H_2. In-cylinder pressure is an important magnitude because its action on the piston during the power stroke produces on the crankshaft the so-called indicated torque [35].

It is clear from Eq. A(7) that the pressure is the result of the combined effects of the adiabatic temperature (T_e) and the change of the number of moles upon combustion ($\sum_P n_e/\sum_R n_i$). As far as the factor $\sum_P n_e/\sum_R n_i$ is the same (pure carbon monoxide, pure hydrogen and 25 % CO–75 % H_2 mixture), the pressure follows the same trend than the one discussed for T_e. However, methane combustion does not suffer from molar contraction, resulting in higher values of $\sum_P n_e/\sum_R n_i$, especially at λ values close to 1 (see Fig. 3). For that reason, the pressure rises much more markedly as λ decreases when burning pure methane and the 80 % CH_4–20 % H_2 mixture compared to other cases. The result is that the highest pressures are obtained with these fuels when the air–fuel equivalence ratio is between 1 and ca. 1.3. Once again, the 20 % CH_4–80 % H_2 mixture shows a behavior intermediate between that of pure methane and pure hydrogen. In contrast, pure carbon monoxide outperforms the other fuels at $\lambda \geq 1.3$ which is interesting because, whereas this compound is not commonly considered as a fuel, it is present in the gases obtained from the thermochemical processing of biomass and in some waste industrial gases.

The fact that the adiabatic temperature was used to calculate the maximum in-cylinder pressure obviously leads to artificially high values; however, it allows understanding in a relatively easy way some of the effects associated to the fuel nature on the combustion process, and on the engine performance, as will be shown in the next section.

3. Automotive engine performance

The engine used in this work is a naturally aspirated PFI four-cylinder VW 1.4 L SI engine. It gives maximum brake power (MBP) and maximum brake torque (MBT) of 59 kW at 5000 rpm and 132 N·m at 3800 rpm, respectively, when gasoline is used as fuel. Its adaptation to run on gaseous fuels and the test bench used in this work have been described in previous papers [15,19,22].

3.1. Experimental conditions and data analysis

Each fuel (pure or binary mixture) has been tested at selected values of λ within their respective flammability limits. All the experiments were performed at full load (WOT) and engine speed of 2000 rpm. During the tests, 200 engine cycles were analyzed after reaching steady conditions. The pressure in cylinder number 1 and brake torque (BT) values were recorded every 0.2° of crank angle (CA). The number of cycles was selected in view of the large cycle-by-cycle variability observed. As an example, Fig. 5 shows the in-cylinder pressure values during 6 cycles when using pure methane as fuel at $\lambda = 1$ and SA of 10° before top dead center (BTDC). Maximum pressure values varied within a wide range; in this case, between ca. 23 bar (misfire) and 51 bar.

Cycle-by-cycle variation is a complex phenomenon that, depending on the engine design and operating variables, is affected to a greater or lesser extent by a variety of factors. Among them, the following stand out: gas motion in the cylinder, variations in the amounts of fuel, air, and residual gases in the cylinder after intake valve closing, mixing effects leading to composition gradients, especially near the spark plug, etc. [35]. The results found in the present work indicate a strong influence of the operating conditions as given by the air-to-fuel equivalence ratio and the spark advance. This is exemplified with the results obtained using methane as fuel that are compiled in Table 2.

Due to the big cycle-by-cycle variations, the brake torque, and then, the resulting mean effective pressure (BMEP), are more reliable metrics to describe the engine operation performance than the in-cylinder pressure. Obviously, as λ increases and the mixture becomes fuel-leaner, both BT and BMEP decrease. As it is well-known, for a given value of λ, the brake torque increases with SA until reaching a maximum value (MBT). Some retard (lower SA) from the optimal value is used in practice to reduce the risk and intensity of knock [35]. SA for MBT increases with λ due to the concomitant reduction of the combustion rate that takes place under increasingly fuel-lean conditions, resulting in an

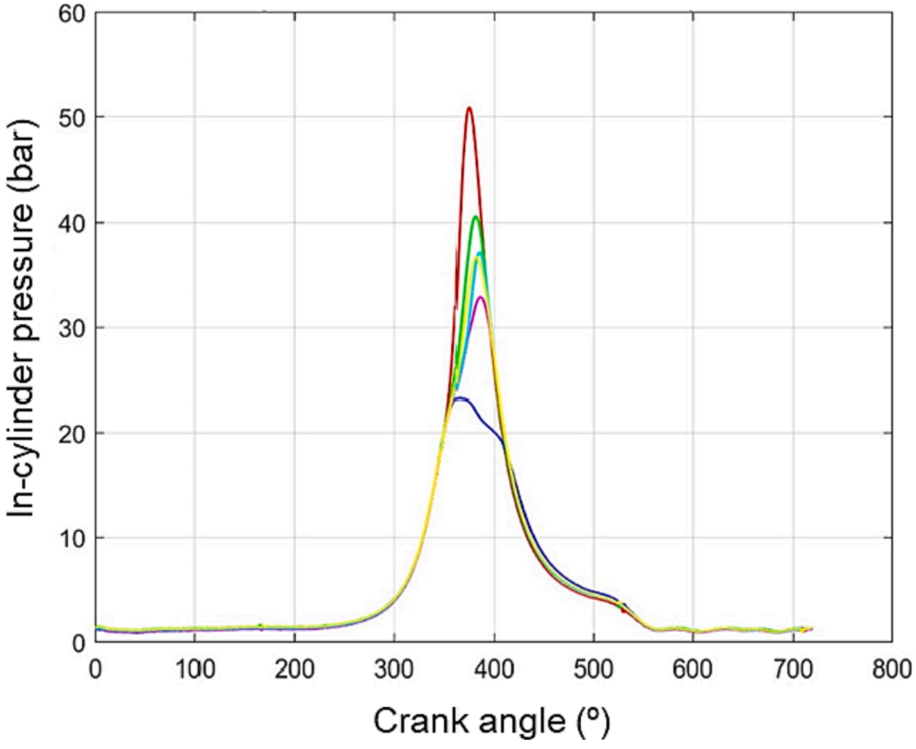

Fig. 5. In-cylinder pressure during six engine cycles as a function of crank angle when using pure methane as fuel ($\lambda = 1$, SA = 10° BTDC, WOT, 2000 rpm).

Table 2
Engine performance using methane as fuel as functions of the air-to-fuel equivalence ratio (λ) and the spark advance (SA).[a]

λ	SA (° BTDC)	Maximum in-cylinder pressure (bar)	Minimum in-cylinder pressure (bar)	Mean in-cylinder pressure (bar)	Standard deviation (bar)	BT (N·m) [b]	BMEP (bar) [c]
1	10	50.92	23.24	34.72	4.61	85	7.6
1	20	59.21	38.98	49.32	3.88	90	8.1
1	30	67.09	52.88	60.52	2.46	84	7.6
1.2	20	46.93	25.14	34.55	4.50	79	7.1
1.2	30	53.49	30.07	44.31	4.57	79	7.1
1.2	40	61.81	32.95	53.19	4.43	76	6.8
1.5	45	74.76	60.76	65.53	3.73	58	5.2
1.5	55	76.14	62.85	66.81	3.79	60	5.4
1.5	65	77.65	65.91	69.15	3.18	57	5.1

[a] Operating conditions: WOT and 2000 rpm. Results recorded throughout 200 engine cycles.
[b] Brake torque.
[c] Brake mean effective pressure; calculated considering a cylinder volume displaced of 1.398 dm^3 according to the engine specifications.

Table 3
Engine performance using the fuels indicated as functions of the air-to-fuel equivalence ratio (λ) and the spark advance (SA).[a]

Fuel	λ	SA (° BTDC)	BT (N·m)	BMEP (bar)
H_2	1.5	10	60	5.4
H_2	1.7	15	55	4.9
H_2	2.0	15	45	4.0
CH_4	1.0	25	89	8.0
CH_4	1.2	30	79	7.1
CO	1.2	25	77	6.9
CO	1.5	40	62	5.6
20 % CH_4–80 % H_2	1.2	10	76	6.8
20 % CH_4–80 % H_2	1.6	30	59	5.3
20 % CH_4–80 % H_2	2.0	35	46	4.1
80 % CH_4–20 % H_2	1.0	30	88	7.9
80 % CH_4–20 % H_2	1.2	35	80	7.2
25 % CO–75 % H_2	1.5	10	62	5.6
25 % CO–75 % H_2	1.7	15	56	5.0
25 % CO–75 % H_2	2.0	20	47	4.2

[a] Operating conditions: WOT and 2000 rpm. Results recorded throughout 200 engine cycles.

increased duration of the fuel burning process in terms of crank angle degrees. Of course, in the same way that each fuel is characterized by some flammability limits and combustion kinetics, it is also distinguished by a given SA for MBT. Table 3 includes the values of λ and SA used with each fuel, as well as the BT and BMEP results obtained.

The values of the air-to-fuel equivalence ratio are affected by the flammability limits but there are also other influencing factors such as the occurrence of anomalous combustion phenomena [16], mainly knock, which is one of the main drawbacks of hydrogen and carbon monoxide as fuels of SI engines [37,38]. For that reason, high values of λ ($\geq$1.5) have been employed with hydrogen-rich fuels only. In the case of methane and, to a lesser extent, carbon monoxide, engine operation could not be extended to the very fuel-lean region because, under those conditions, the combustion reaction was not complete [15,19]. Therefore, lean operation was limited at $\lambda = 1.2$ for pure methane and $\lambda = 1.5$ for pure carbon monoxide. The binary mixtures combined the characteristics of each component. As a result, the methane-hydrogen mixtures allowed to operate within a wide range of λ, with values varying between 1 (80 % CH_4–20 % H_2) and 2 (20 % CH_4–80 % H_2). On the other hand, the carbon monoxide-hydrogen mixture could be burned at very lean conditions thanks to its high hydrogen molar content. Regarding the SA for MBT, it can be seen in Table 3 that, for a given fuel, the advance increases with λ. It should be noted that the rate of the combustion reactions decreases as the fuel concentration becomes lower when λ increases. For that reason, SA has to increase to allow for complete combustion, especially for methane, the fuel most difficult to burn of the three considered in this study.

3.2. Results discussion

It is evident that there are enormous differences between the maximum combustion pressures calculated theoretically (Fig. 4) and the values recorded during engine operation (Table 2 and Table 3). There are many important phenomena not considered by the simple thermodynamic model formulated that are affecting the experimental results. In addition to heat transfer to the cylinder walls and piston head, incomplete combustion and kinetic and fluid dynamics aspects (flame speed, turbulence-induced effects, etc.), indicated power, mechanical friction and pumping work also reduce the engine performance [33]. Despite these considerations, it is interesting to compare the theoretical and experimental results, as shown in Fig. 6. There is a clear parallelism between the maximum theoretical combustion pressure and BMEP. Note that BMEP is derived directly from the experimental data of BT and the engine speed and cylinder volume displaced. It is remarkable that, despite their different nature, the fuels approximately fall into the same trend lines. This indicates that the nature of the fuel mainly affects the value of λ at which the engine can be operated, whereas λ itself governs the performance of the engine.

Achieving a better performance requires close to stoichiometric conditions that can be met with pure methane or methane blended with hydrogen in relatively low molar concentration. On the other hand, very lean operation ($\lambda \geq 1.5$) is possible with pure hydrogen or hydrogen blended with methane or carbon monoxide in low molar concentrations. Considering intermediate values of the air-to-fuel equivalence ratio (e.g., $1.6 \geq \lambda \geq 1.3$) as a compromise solution, they can be achieved on the fuel-lean region with pure hydrogen, and hydrogen-rich blends with carbon monoxide (25 % CO–75 % H_2) and methane (20 % CH_4–80 % H_2). On the other hand, the fuel-rich limit can be achieved with pure carbon monoxide and methane-rich blends with hydrogen (80 % CH_4–20 % H_2). This last mixture allows running the engine under the widest range of λ (1.2–2).

As judged from the slopes of the respective trend lines in Fig. 6, the divergence among the results increases as λ approaches stoichiometric conditions. It seems likely that this is due to the model's assumption of instantaneous (and complete) combustion. In other words, the experimental work has been performed adjusting the SA for MBT for every case, which implies considering the combustion kinetics features of each fuel at given mixture composition (λ). Nevertheless, the strong correlation existing between the experimental and the theoretical parameters can be clearly seen in Fig. 7. Relative standard deviation is within 2.1 %–4.2 %.

The simplifications underpinning the thermodynamic model developed greatly limit its predictive capability. However, it allows to see clearly that, as naturally aspirated PFI SI engines running on gaseous fuels are concerned, λ is the key parameter governing the engine performance if SA is optimized. The gaseous fuels nature is important as it defines the range of λ values that can considered to operate safely the

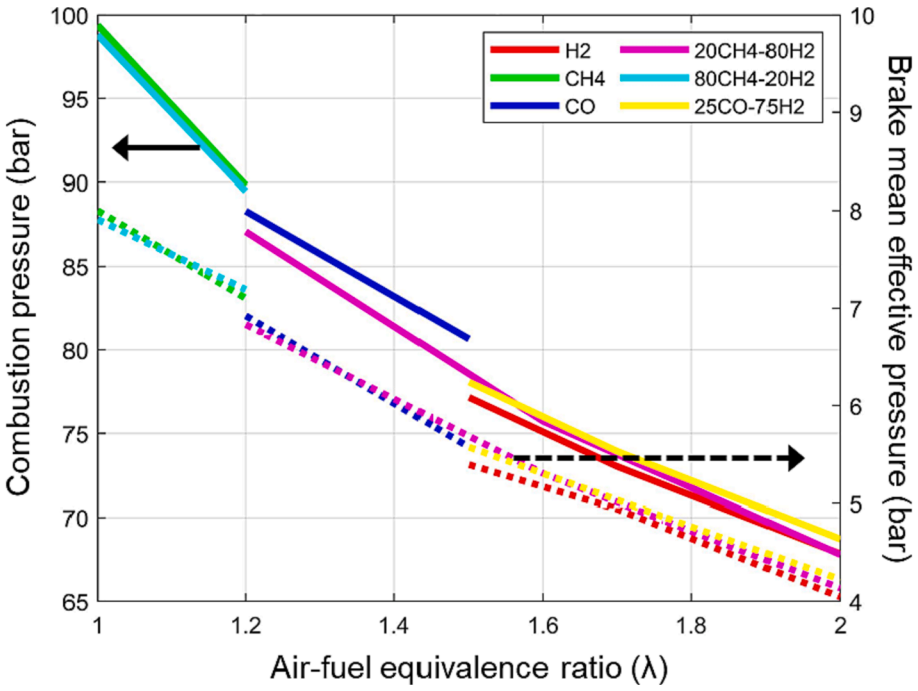

Fig. 6. Pressure of the combustion products according to Eq. A(7) (solid lines) and BMEP (dotted lines) as functions of the air–fuel equivalence ratio for the fuels indicated. Engine operated at WOT, 2000 rpm and SA for MBT.

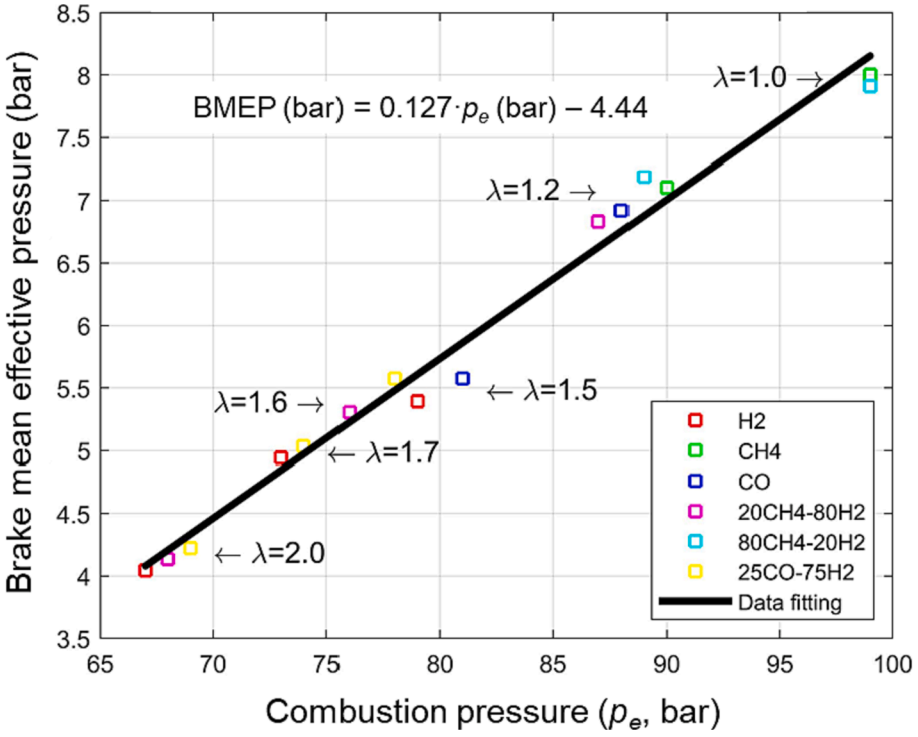

Fig. 7. Correlation between the experimental brake mean effective pressure (BMEP) and the pressure of the combustion products according to Eq. A(7) (p_e) for the fuels and λ values indicated. Engine operated at WOT, 2000 rpm and SA for MBT.

engine free of abnormal combustion phenomena or other problems such as incomplete combustion. However, as far as a λ value is achievable with various fuels, their composition is of minor importance regarding MBT (and then BMEP).

Caton arrived to a similar conclusion through interesting first and second laws engine cycle simulation studies considering stoichiometric conditions ($\lambda = 1$) and a variety of fuels including both gaseous and liquid organic compounds (hydrogen, carbon monoxide, methane, propane, hexane, isooctane, methanol and ethanol) [32,33]. Application of first law led to very similar engine performance parameters for the several fuels. Main differences arose from the perspective of the second law; more specifically, from the exergy destroyed during the combustion process for the various fuels. In this regard, carbon monoxide showed the lowest exergy destruction whereas isooctane exhibited the highest

Table 4
Specific fuel consumption as function of the air-to-fuel equivalence ratio (λ).[a]

Fuel	λ	Fuel flow rate (m^3/h) [b]	Brake power (kW)	BSFC [c] (g/kW·h)	Volumetric consumption (m^3/kW·h) [b]
H_2	1.5	14.31	12.56	102.5	1.14
H_2	1.7	13.00	11.52	101.6	1.13
H_2	2.0	10.40	9.42	99.4	1.10
CH_4	1.0	6.90	18.64	265.1	0.37
CH_4	1.2	5.99	16.54	258.9	0.36

[a] Operating conditions: WOT and 2000 rpm.
[b] Flow rate and volume are referred to 1 atm and 273.15 K.
[c] Brake specific fuel consumption.

one. These results were correlated with the nature (composition and complexity) of the fuel molecule. Simple molecules (hydrogen), specially containing oxygen (carbon monoxide), lead to lower exergy destruction. Moreover, in these two cases, the entropy increase is moderated by the reduction of the number of moles upon the combustion reaction. In contrast, the combustion of complex molecules containing multiple carbon–carbon bonds and without oxygen atoms destroys more exergy. A similar interpretation has been given by Rakopoulos et al. for the case of hydrogen [39]. According to these authors, hydrogen combustion is distinguished by the fact that it resembles more to a recombination process between simple molecules than to the destruction of complex molecules occurring during the combustion of other fuels. As a matter of fact, the combustion product (water) is a more complex molecule than the reactants. This is advantageous from the point of view of the second law. The same arguments are valid for the combustion of CO.

Another important aspect to be considered is the consumption of fuel in relation to the engine performance. Brake power and brake specific fuel consumption (BSFC) results when the engine is fueled with methane and hydrogen at different values of λ are compiled in Table 4.

In both cases, the BSFC slightly decreases as λ increases due to the efficiency increase associated to fuel-lean operation. On the other hand, the BSFC is significantly higher (ca. 2.6 times) for methane combustion than for hydrogen combustion. As discussed before for the adiabatic temperature values shown in Fig. 1, these results should be linked to the lower LHV of methane compared to hydrogen (2.4 times lower at standard conditions, see Table 1). Actually, the situation is reversed if the volumetric fuel consumption is considered (Table 4). Indeed, the volumetric consumption of hydrogen is ca. 3.1 times higher than that of methane referred to standard temperature and pressure conditions, in accordance with the lower molar heating value of hydrogen compared to methane (ca 3.3 times, see Table 1). Taking into account their respective LHVs, brake thermal efficiencies within 27.2 %-27.8 % and 29.3 %-30.2 % result for pure methane and hydrogen, respectively, under the operating conditions indicated in Table 4. These results are in line with previous experimental and numerical studies [19,40].

4. Summary and conclusions

Main outcomes of this thermodynamic and experimental study have shown that the performance parameters (i.e., BT and BMEP) of a naturally aspirated automotive SI engine are very similar when using methane, carbon monoxide, hydrogen and some of their mixtures as fuels provided that the air–fuel equivalence ratio (λ) employed is the same. The work has been performed adjusting in each case the SA in order to obtain MBT at full load and engine speed of 2000 rpm. Overall, the fuels considered have allowed to operate the engine between stoichiometric ($\lambda = 1$) and fuel-lean conditions ($\lambda = 2$). It should be highlighted that no fuel (pure or blend) could be used covering the whole range of λ values indicated, though the 20 % CH_4–80 % H_2 blend allowed to operate the engine within a broad window ($1.2 < \lambda < 2$). The stoichiometric limit was problematic for fuels such as hydrogen and hydrogen-rich mixtures, prone to suffer from knock. On the other hand, very lean conditions led to incomplete combustion of the fuels (methane and methane-rich mixtures) characterized by slower combustion kinetics. Carbon monoxide showed a behavior intermediate between those of methane and hydrogen. Therefore, within the limits of the present study, it can be concluded that the fuel nature conditioned the composition of the mixture with air that could be burned. Another significant outcome of the present study is that a simple first-law zero-dimensional model is capable of describing reasonably well the trends marked by the experimental results, though the simplifications made greatly limit its predictive capability.

This work illustrates the interest of using methane, carbon monoxide, hydrogen and their blends as fuels of SI engines. As these gases can be obtained from renewable resources, their use in ICEs is a clear opportunity to support the decarbonization of the transport sector as well as the distributed generation of electricity through engine-generators.

CRediT authorship contribution statement

José Carlos Urroz: Data curation, Methodology. **Pedro M. Diéguez:** Conceptualization, Resources, Methodology. **Gurutze Arzamendi:** Data curation. **Miguel Arana:** Data curation, Formal analysis. **Luis M. Gandía:** Conceptualization, Writing – review & editing.

Declaration of Competing Interest

The authors declare that they have no known competing financial interests or personal relationships that could have appeared to influence the work reported in this paper.

Data availability

Data will be made available on request.

Acknowledgements

Financial support from Spanish Ministerio de Ciencia e Innovación and Agencia Estatal de Investigación MCIN/AEI/10.13039/501100011033/ and FEDER “Una manera de hacer Europa” (grant PID2021-127265OB-C21), as well as from Plan de Recuperación, Transformación y Resiliencia and NextGenerationEU (grants PLEC2022-009221 and TED2021-130846B-100) is gratefully acknowledged. L.M. Gandía also thanks Banco de Santander and Universidad Pública de Navarra for their financial support under “Programa de Intensificación de la Investigación 2018” initiative. Authors also acknowledge Open Access Funding provided by Universidad Pública de Navarra.

Appendix

The first law of thermodynamics applied to the combustion of a fuel can be written as follows:

$$0 = \sum_P n_e u_e(T_e) - \sum_R n_i u_i(T_i) \quad \text{(A1)}$$

where n_i $[i = 1\cdots R]$ and n_e $[e = 1\cdots P]$ are the number of moles of reactants and products, respectively, which are considered to behave as ideal gases. Therefore, the specific internal energy of a given compound $u(T)$ only depends on temperature (T), that is assumed homogeneous inside the cylinder volume delimiting the thermodynamic system under study (single zone model).

The following general combustion reaction can be written for a hypothetical mixture containing α moles of hydrogen, β moles of methane, γ moles of carbon monoxide, δ moles of nitrogen and ε moles of carbon monoxide assuming that the molar composition of air is 21 % oxygen and 79 % nitrogen:

$$\alpha H_2+\beta CH_4+\gamma CO+\delta N_2+\varepsilon CO_2+\lambda\left(\frac{\alpha}{2}+2\beta+\frac{\gamma}{2}\right)\left(O_2+\frac{79}{21}N_2\right)\rightarrow(\alpha+2\beta)H_2O+(\beta+\gamma+\varepsilon)CO_2+(\lambda-1)\left(\frac{\alpha}{2}+2\beta+\frac{\gamma}{2}\right)O_2+\left[\lambda\frac{79}{21}\left(\frac{\alpha}{2}+2\beta+\frac{\gamma}{2}\right)+\delta\right]N_2 \tag{A2}$$

Where λ is the air–fuel equivalence ratio that is defined as the quotient between the actual mass air–fuel ratio *(AF)* of the mixture loaded into the cylinders and the mass air–fuel ratio corresponding to stoichiometric conditions $(AF)_{stoich}$:

$$\lambda=(AF)/(AF)_{stoich} \tag{A3}$$

Values of λ lower than 1 correspond to fuel-rich mixtures, values of λ higher than 1 correspond to fuel-lean mixtures and $\lambda = 1$ stands for a mixture in which fuel and air are in stoichiometric proportion.

Application of Eq. A(1) to the combustion of the above-mentioned mixture leads to:

$$0=\left\{[\alpha+2\beta]\cdot u_{H_2O}(T_e)+[\alpha+\beta+\varepsilon]\cdot u_{CO_2}(T_e)+\left[(\lambda-1)\left(\frac{\alpha}{2}+2\beta+\frac{\gamma}{2}\right)\right]\cdot u_{O_2}(T_e)+\left[\lambda\frac{79}{21}\left(\frac{\alpha}{2}+2\beta+\frac{\gamma}{2}\right)+\delta\right]\cdot u_{N_2}(T_e)\right\}-\left\{\alpha\cdot u_{H_2}(T_i)+\beta\cdot u_{CH_4}(T_i)+\gamma\cdot u_{CO}(T_i)+\varepsilon\cdot u_{CO_2}(T_i)+\left[\lambda\left(\frac{\alpha}{2}+2\beta+\frac{\gamma}{2}\right)\right]\cdot u_{O_2}(T_i)+\left[\lambda\frac{79}{21}\left(\frac{\alpha}{2}+2\beta+\frac{\gamma}{2}\right)+\delta\right]\cdot u_{N_2}(T_i)\right\} \tag{A4}$$

The internal energy of the several compounds has been calculated according to Eq. A(5):

$$u(T)=h(T)-R\cdot T=h_f^0+\Delta h(T)-R\cdot T \tag{A5}$$

Where h_f^0 is the specific enthalpy of formation at the reference conditions of 298 K and 1 atm, $\Delta h(T)$ is the change of specific enthalpy with respect to that state, and R the universal gas constant. In the present work, all the thermodynamic properties have been calculated using the REFPROP program from NIST [34].

As for the reactants temperature (T_i), it has been taken as the in-cylinder value at the end of the compression stroke calculated according to:

$$T_i=T_a\cdot(p_i/p_a)\cdot(1/r_c) \tag{A6}$$

Where p_i is the in-cylinder pressure at the end of the compression stroke, T_a and p_a are the temperature and pressure in the intake manifold, respectively, and r_c the cylinder compression ratio. Values for these variables have been taken from the characteristics and unthrottled operation of the SI naturally aspirated automotive engine used in this work, so that $r_c = 10.5$, T_a= 303 K and $p_a = 0.93$ bar. Regarding p_i, tests were carried out consisting of operating the engine driven only by the electric starter engine, in absence of spark ignition, recording the maximum in-cylinder pressure resulting in a mean value of 22.2 bar. Therefore, application of Eq. A(6) gives $T_i = 689$ K, which allows calculating T_e for the combustion of a fuel(s)-air mixture of given composition.

Finally, as the combustion reaction is considered to take place being the volume constant, the resulting in-cylinder pressure has been calculated as follows:

$$p_e=p_i\cdot\left(\sum_P n_e/\sum_R n_i\right)\cdot(T_e/T_i) \tag{A7}$$

where $\left(\sum_P n_e/\sum_R n_i\right)$ is the ratio between the total number of moles of products and reactants in the cylinder, or after and before the combustion reaction, respectively.

References

[1] Glasgow Climate Pact. Conference of the Parties serving as the meeting of the Parties to the Paris Agreement. Third session. Glasgow, 31 October to 12 November 2021. https://unfccc.int/sites/default/files/resource/cma2021_L16_adv.pdf.

[2] IEA, Key World Energy Statistics 2021, IEA Publications, International Energy Agency, France, September 2021.

[3] IEA (2021), Greenhouse Gas Emissions from Energy: Overview, IEA, Paris https://www.iea.org/reports/greenhouse-gas-emissions-from-energy-overview.

[4] Olivier JGJ, Peters JAHW. Trends in global CO_2 and total greenhouse gas emissions: 2020 Report. The Hague: PBL Netherlands Environmental Assessment Agency; 2020.

[5] Ursúa A, Gandía LM, Sanchis P. Hydrogen production from water electrolysis: current status and future trends. Proc IEEE 2012;100:410–26. https://doi.org/10.1109/JPROC.2011.2156750.

[6] Gandía LM, Arzamendi G, Diéguez PM, editors. Renewable hydrogen technologies. Amsterdam: Elsevier B.V; 2013.

[7] European Commission. A hydrogen strategy for a climate-neutral Europe. Brussels: 8.7.2020. COM(2020) 301 final.

[8] IRENA. Global Renewables Outlook: Energy transformation 2050. International Renewable Energy Agency. Abu Dhabi: 2020.

[9] Hydrogen Europe. H2ero Net Zero. Hydrogen Europe Position Paper. Unlocking the potential of clean mobility: the revision of CO_2 emission standards for cars and vans. July 2021.

[10] Fuel Cells and Hydrogen 2 Joint Undertaking. Hydrogen Roadmap Europe. Belgium; January 2019.

[11] Verhelst S, Wallner T. Hydrogen-fueled internal combustion engines. Prog Energy Combust Sci 2009;35:490–527. https://doi.org/10.1016/j.pecs.2009.08.001.

[12] Stępień Z. A comprehensive overview of hydrogen-fueled internal combustion engines: achievements and future challenges. Energies 2021;14:6504. https://doi.org/10.3390/en1420650.

[13] Hosseini SE, Butler B. An overview of development and challenges in hydrogen powered vehicles. Int J Green Energy 2020;17:13–37. https://doi.org/10.1080/15435075.2019.1685999.
[14] Sinigaglia T, Lewiski F, Martins MES, Siluk JCM. Production, storage, fuel stations of hydrogen and its utilization in automotive applications-a review. Int J Hydrog Energy 2017;42:24597–611. https://doi.org/10.1016/j.ijhydene.2017.08.063.
[15] Diéguez PM, Urroz JC, Marcelino-Sádaba S, Pérez-Ezcurdia A, Benito-Amurrio M, Sáinz D, et al. Experimental study of the performance and emission characteristics of an adapted commercial four-cylinder spark ignition engine running on hydrogen–methane mixtures. Appl Energy 2014;113:1068–76. https://doi.org/10.1016/j.apenergy.2013.08.063.
[16] Diéguez PM, Urroz JC, Sáinz D, Machin J, Arana M, Gandía LM. Characterization of combustion anomalies in a hydrogen-fueled 1.4 L commercial spark-ignition engine by means of in-cylinder pressure, block-engine vibration, and acoustic measurements. Energy Convers Manag 2018;172:67–80. https://doi.org/10.1016/j.enconman.2018.06.115.
[17] Lechner R, Hornung A, Brautsch M. Prediction of the knock propensity of biogenous fuel gases: Application of the detonation theory to syngas blends. Fuel 2020;267:117243. https://doi.org/10.1016/j.fuel.2020.117243.
[18] Fischer M, Jiang X. An assessment of chemical kinetics for bio-syngas combustion. Fuel 2014;137:293–305. https://doi.org:10.1016/j.fuel.2014.07.081.
[19] Ortiz-Imedio R, Ortiz A, Urroz JC, Diéguez PM, Gorri D, Gandía LM, et al. Comparative performance of coke oven gas, hydrogen and methane in a spark ignition engine. Int J Hydrog Energy 2021;46:17572–86. https://doi.org/10.1016/j.ijhydene.2019.12.165.
[20] Sáinz D, Diéguez PM, Urroz JC, Sopena C, Guelbenzu E, Pérez-Ezcurdia A, et al. Conversion of a gasoline engine-generator set to a bi-fuel (hydrogen/gasoline) electronic fuel-injected power unit. Int J Hydrog Energy 2011;36:13781–92. https://doi.org:10.1016/j.ijhydene.2011.07.114.
[21] Sáinz D, Diéguez PM, Sopena C, Urroz JC, Gandía LM. Conversion of a commercial gasoline vehicle to run bi-fuel (hydrogen-gasoline). Int J Hydrog Energy 2012;37:1781–9. https://doi.org/10.1016/j.ijhydene.2011.10.046.
[22] Sopena C, Diéguez PM, Sáinz D, Urroz JC, Guelbenzu E, Gandía LM. Conversion of a commercial spark ignition engine to run on hydrogen: Performance comparison using hydrogen and gasoline. Int J Hydrog Energy 2010;35:1420–9. https://doi.org:10.1016/j.ijhydene.2009.11.090.
[23] Arana M, San Martín R, Urroz JC, Diéguez PM, Gandía LM. Acoustic and psychoacoustic levels from an internal combustion engine fueled by hydrogen vs. gasoline. Fuel 2022;317:123505. https://doi.org/10.1016/j.fuel.2022.123505.
[24] Fischer M, Sterlepper S, Pischinger S, Seibel J, Kramer U, Lorenz T. Operation principles for hydrogen spark ignited direct injection engines for passenger car applications. Int J Hydrog Energy 2022;47:5638–49. https://doi.org/10.1016/j.ijhydene.2021.11.134.
[25] Kravos A, Seljak T, Oprešnik SR, Katrašnik T. Operational stability of a spark ignition engine fuelled by low H_2 content synthesis gas: Thermodynamic analysis of combustion and pollutants formation. Fuel 2020;261:116457. https://doi.org/10.1016/j.fuel.2019.116457.
[26] Thawko A, Eyal A, Tartakovsky L. Experimental comparison of performance and emissions of a direct-injection engine fed with alternative gaseous fuels. Energy Convers Manag 2022;251:114988. https://doi.org/10.1016/j.enconman.2021.114988.
[27] Shrestha SOB, Narayanan G. Landfill gas with hydrogen addition – A fuel for SI engines. Fuel 2008;87:3616–26. https://doi.org/10.1016/j.fuel.2008.06.019.
[28] He Z, Gao Z, Zhu L, Li S, Li A, Zhang W, et al. Effects of H_2 and CO enrichment on the combustion, emission and performance characteristics of spark ignition natural gas engine. Fuel 2016;183:230–7. https://doi.org/10.1016/j.fuel.2016.06.077.
[29] Lather RS, Das LM. Performance and emission assessment of a multicylinder S.I engine using CNG & HCNG as fuels. Int J Hydrog Energy 2019;44:21181–92. 10.1016/j.ijhydene.2019.03.137.
[30] Roy MM, Tomita E, Kawahara N, Harada Y, Sakane A. Performance and emissions of a supercharged dual-fuel engine fueled by hydrogen-rich coke oven gas. Int J Hydrog Energy 2009;34:9628–38. https://doi.org/10.1016/j.ijhydene.2009.09.016.
[31] Verhelst S, Sheppard CGW. Multi-zone thermodynamic modelling of spark-ignition engine combustion – An overview. Energy Convers Manag 2009;50:1326–35. https://doi.org/10.1016/j.enconman.2009.01.002.
[32] Caton JA. An introduction to thermodynamic cycle simulations for internal combustion engines. Chichester: John Wiley & Sons; 2016.
[33] Caton JA. Implications of fuel selection for an SI engine: Results from the first and second laws of thermodynamics. Fuel 2010;89:3157–66. https://doi.org/10.1016/j.fuel.2010.05.005.
[34] NIST Reference Fluid Thermodynamic and Transport Properties Database (REFPROP): Version 10. Available at https://www.nist.gov/srd/refprop.
[35] Heywood JB. Internal combustion engine fundamentals. New York: McGraw-Hill, Inc.; 1988.
[36] Glassman I, Yetter RA. Combustion. 4th Ed. Amsterdam: Academic Press-Elsevier; 2008.
[37] Malenshek M, Olsen DB. Methane number testing of alternative gaseous fuels. Fuel 2009;88:650–6. https://doi.org/10.1016/j.fuel.2008.08.020.
[38] Diaz GJA, Corredor Martinez LM, Gomez Montoya JP, Olsen DB. Methane number measurements of hydrogen/carbon monoxide mixtures diluted with carbon dioxide for syngas spark ignited internal combustion engine applications. Fuel 2019;236:535–43. https://doi.org/10.1016/j.fuel.2018.09.032.
[39] Rakopoulos CD, Scott MA, Kyritsis DC, Giakoumis EG. Availability analysis of hydrogen/natural gas blends combustion in internal combustion engines. Energy 2008;33:248–55. https://doi.org/10.1016/j.energy.2007.05.009.
[40] Ortiz-Imedio R, Ortiz A, Ortiz I. Comprehensive analysis of the combustion of low carbon fuels (hydrogen, methane and coke oven gas) in a spark ignition engine through CFD modeling. Energy Convers Manag 2022;251:114918. https://doi.org/10.1016/j.enconman.2021.114918.